Journal of
Ship&Ocean
Technology

SOTECH Vol. 8, No. 2, pp. 20~28, 2004

Dynamic-Thermodynamic Sea Ice Model: Application to Climate Study and Navigation

Alexander P. Makshtas[1], Serger V. Shoutilin[1], Alexey V. Marchenko[1] and Roman V. Bekryaev[1]

[1] International Arctic Research Center, University of Alaska Fairbanks, USA;
E-mail: makshtas@iarc.uaf.edu

Abstract

A dynamic–thermodynamic sea ice model with 50-km spatial and 24-hour temporal resolution is used to investigate the spatial and long-term temporal variability of the sea ice cover the Arctic Basin. The model satisfactorily reproduces the averaged main characteristics of the sea ice and the sea ice extent in the Arctic Basin and its decrease in early 1990th. At times model allows to suppose partial recovery of sea ice cover in the last years of twenty century. The employment of explicit form for description of ridging gives opportunity to assume that the observed thinning is the result of reduction the intensity of ridging processes and to estimate long-term variability of probability the ridge free navigation in the different parts of the Arctic Ocean including the North Sea Route area.

Keywords: sea ice ridges, spatial-temporal variability, Arctic Ocean, navigation

1 Introduction

Recent reports of the decrease in sea ice extent in early 1990th (e.g. Parkinson et al 1999) and thickness (Rothrock et al 1999) in the Arctic Basin stimulate attempts to explain this remarkable change in the main features of the Arctic climate system. One of the main ways to understand the reasons for climate changes is to use numerical modeling to reproduce observed environmental characteristics and to study the possible mechanisms responsible for such changes. Explanation of these changes, however, depends crucially on the model used for investigating and the external forcing applied in the model. Many authors (e.g. Maslanik et al 2000) explain the decrease in sea ice cover in the eastern part of the Arctic Ocean during last decades as a consequence of increased open water and thin ice, forced primarily by ice dynamics. As a result, the surface albedo decreases; the absorbed solar radiation at the surface and in the oceanic mixed layer likewise increases; and, finally, the lateral and bottom melting increases. Hilmer and Lemke(2000), on the other hand, conclude from sensitivity simulations that most of the thinning can be attributed to changes in the surface-level air temperature rather than to changes in the circulation.

Using Thorndike's (1992) simple model, Rothrock et al(1999) discussed possible thermodynamic processes that could produce the observed thinning, such as an increase in the oceanic heat flux, an increase in the poleward atmospheric heat transport and the consequent increase in the incoming longwave radiation, or an increase in the downwelling shortwave radiation. Some support for this last hypothesis is contained in the paper of Ikeda et al(2002), based on data of meteorological and radiation observations from the North Pole drifting stations. Other proposed reasons for the decrease in sea ice thickness and extent are changes in snow precipitation and snow depth (Warren et al 1999) or an increase in ice export from the Arctic Basin (Kwok and Rothrock 1999).

In our previous papers (Makshtas et al 2002, 2003) we argued that the observed decrease of sea ice cover in early 1990th is the result of reduction the intensity of ridging processes due to dynamic reasons, namely due to intensification of atmospheric cyclonic circulation above the Arctic Basin (Polyakov and Johnson 2000). Further numerical experiments with extended up to 2002 NCEP/NCAR reanalysis data (Kalnay et al 1996), the main external forcing in the model, allow to presupposes that in the end of twenty century sea ice in the Arctic Ocean partly recovered, at least in the Canadian Arctic. Such suggestion is supported partly by results obtained by Tucker et al (2001), Winsor (2001), and Rothrock et al (2003). Follow our model (Makshtas et al, 2003) it was due to intensification of ridging processes due to changes in atmospheric circulation from cyclonic to anticyclonic.

It is well known that ridges are the one of the main obstacles for navigation in ice-covered seas. Additionally to investigations of climatic behavior of sea ice cover our model with simplified explicit description of ridging gives us possibility to estimate the long-term variation of probability of ridge free navigation in the different parts of the Arctic Ocean, including the North Sea Route area. In this paper we analyze the results of calculations the spatial-temporal redistribution of level ice thickness and ridge concentration derived with a dynamic-thermodynamic model forced by atmospheric data from 1948-2001 to study the long-term variability of the Arctic sea ice cover in application to some aspects of navigation in the Arctic seas.

2 Model

The sea ice cover in our large-scale dynamic-thermodynamic model (Makshtas et al 2003) is described at each grid point by the relative areas of level or undeformed ice (thickness h_i, area N_i), which undergoes thermodynamic growth and melting; ridged ice (area N_h) with fixed effective thickness h_h=12 m, and leads (area N_0). The main equations of the model are the momentum equation, which includes a parameterization of internal ice stresses in the framework of a cavitating fluid (Flato and Hibler 1992); the quasi-steady heat conduction equation, which describes heat processes in the level sea ice and its growth or melting; and the nonstationary mass balance equation. This last equation is

$$\frac{\partial m_i}{\partial t} + div(\vec{u} m_i) + f = 0 \qquad (1)$$

where $m_i = h_i N_i + h_h N_h$ and $\vec{u}$ is ice drift velocity. Finally, here,

$$f = N_i \left(\frac{\partial h_i}{\partial t} \right)_T + h_i \left(\frac{\partial N_i}{\partial t} \right)_T + h_h \left(\frac{\partial N_h}{\partial t} \right)_T + N_h \left(\frac{\partial h_h}{\partial t} \right)_T \qquad (2)$$

is a function describing thermodynamic growth or melting of level ice, lateral melting of level and ridged ice in leads, and melting at the upper and lower surfaces of ridges, recalculated in turn to reduction of area occupied by ridged ice and increase the area occupied by level ice.

Our model describes the growth and melting of level ice with a zero-dimensional thermodynamic sea ice model, similar to Semtner's (1976) model. We describe the energy fluxes between the atmospheric surface layer and sea ice surface following Jordan et al (1999). We model heat processes in leads following Ebert and Curry (1993). To calculate the redistribution of lateral heat fluxes between ridged and level ice, we use an algorithm proposed by Doronin (1969). We describe the bottom and surface melting of ridges following Thorndike et al (1975, their Table 1).

Determined by (1) redistribution of the areas occupied by leads, level ice, and ridges in each cell is calculated with an algorithm based on the method of large particle (Belotserkovskii 1984) and the obvious relation

$$N_0 + N_i + N_h = 1 \tag{3}$$

Following Belotserkovskii (1984), we integrate (1) in three steps. In the first (Eulerian) step the values within the cell as a whole are estimated assuming solid-body movement. In the second (Lagrangian) step, the transfer of properties between cells is calculated under the assumption that properties are carried across cell boundaries with the components of drift velocity normal to the boundary. Finally, in the last step, the grid is reformed, all calculated parameters are redistributed on it, and Eulerian distributions of parameters in the initial grid for $t^{n+1}=t^n+\Delta t$ are determined. When convergence of ice drift velocity takes place, additional areas of level ice and ridges coming into the cell from surrounding cells can lead to a situation in which the new total area of level ice and ridges exceeds the cell area. Then final N_i^f and N_h^f are calculated from the following equations, which imitate ridging processes:

$$N_i^f + N_h^f = 1 \qquad N_i h_i + N_h h_h = N_i^f h_i + N_h^f h_h \tag{4}$$

The model is driven using daily 2-meter air temperature and relative humidity, atmospheric surface pressure, total cloudiness amount, monthly mean solid precipitation and dynamic heights of the ocean surface. The model has a horizontal resolution of 50 km by 50 km and a temporal resolution of 24 hours. With the model, we can calculate the temporal-spatial distributions of the level sea ice thickness and area, ridges and leads areas, the snow depth, the turbulent sensible (H) and latent (LE) heat fluxes, longwave (R) and shortwave (F) radiation balances at the upper surface for each kind of ice cover, the temperature in leads and in the upper ocean, and the heat flux from the oceanic mixed layer to the bottom of the sea ice.

For future consideration it needs to emphasize that the simplest rectangular shape of ridges with fixed height equal to 12 meters was used in our model. Shortly model reproduces the volume of ridged ice in each cell only. For estimation the number of ridges in the unit of area we must use typical values of the ridge cross-section area and length of single ridge. The first value we calculate using data about geometrical parameters of ridge cross-section from Burden and Timco (1995), constructed typical profiles of ridge from the data of more than 250 sets of measurements. The generalization of their results gives the mean value of ridge cross-section area about 190 m^2 with variations from 100 m^2 to 250 m^2.

The data about lateral ridge extent even are much more scare. Hibler and Ackley (1973) described the difficulties of ridge extent estimations due to technical problems, as well as some subjective judgments about definition the height cutoff, which must be applied to obtain the ridge length distributions. Refereed to paper for descriptions of methods which had been used for estimations, and based on their final conclusion that examination of available aerial photographs and field observations suggests that the mean ridge length increases slightly with increasing height, and may be of the order of 2 km for 8 to 9-ft ridges and 1 km for 3 to 4-ft ridges as well as on their Figures A1, A2, constructed for the northern part of the Beaufort Sea we use in our model the value 1 km for typical ridge length.

3 Spatial-temporal variability of sea ice in the Arctic Ocean

In our previous papers (Makshtas et al, 2002, 2003) we investigated spatial-temporal variability of sea ice cover in the Arctic Basin during 1959-1997 and its sensitivity to external forcing. The comparison of modeled sea ice with available data showed the good agreement in ice extent, spatial distributions of level ice thickness and ridged area, and ice flux through the Fram Strait. It was found, that atmospheric dynamic and related ridging processes determine the main changes in characteristics of sea ice cover and increase of air surface temperature during investigated period determined only 20% of ice thickness decrease in the Canadian region of Arctic Ocean. Same time we pointed out the small changes in ice volume after 1993. Due to recent extension of NCEP Reanalysis data from 1948 up to 2002, we have possibility now to investigate changes in the arctic sea ice cover for longer period.

Figure 1 presents spatial distributions of level sea ice thickness and number of ridges per unit area. The last values were recalculated from original model using available data about geometry of ridges, described in part 2. The first two periods of averaging (1984-1988, 1989-1993) had been choused, as the periods with mainly dominant anticyclonic and cyclonic circulation of the polar atmosphere (Proshutinsky and Johnson 1997). The last period of averaging (1999-2001) had been choused as a maximal approach to present.

As it was shown by Makshtas et al (2003) during periods with anticyclonic circulation the yearly averaged ice volume in the Arctic Ocean and especially in the Canadian region systematically grows; while during the cyclonic regime, its mainly shrinks. Our results confirm the conclusion by Walsh et al (1996) that dominant cyclonic geostrophic winds tend to increase divergent ice motion in contrast to dominant anticyclonic winds. These circumstances, in turn "would reduce the fractional concentration of multiyear ice and increase the fractional coverage of first year ice in the central Arctic during winter." Our model likewise shows that such changes in the atmospheric circulation lead to decrease the intensity of ridging in the Canadian Basin and adjacent parts of the central Arctic as well as in the marginal seas. This decrease causes on average the thinning of sea ice in early 1990^{th}, when cyclonic circulation in the polar atmosphere was well developed.

Figure 1 shows partial recover of modeled level sea ice thickness in the Canadian region in (1999-2001), especially noticeable in May, the month of maximal seasonal ice thickness. It corresponds to change of atmospheric circulation from cyclonic to anticyclonic after 1996 (Polyakov and Johnson 2000). Same time in the Eurasian region the small decrease of level sea ice thickness could be mentioned. The most remarkable is the temporal variability of ridged ice. In 1989-1993 the ridges number decreased relatively 1984-1988 more than two times, especially in the central part of the Canadian region. It was accompanied by insignificant increasing of ridge number along the north coast of the

Greenland. In 1999-2001 the modeled number of ridges was almost the same as in 1984-1988, and even larger in the northeastern part of the Beaufort Sea. Our results support Rothrock et al (2003) conclusion about absence of any convincing argument that the decline of sea ice thickness through 1996 should be extrapolated as a prediction of its future behavior.

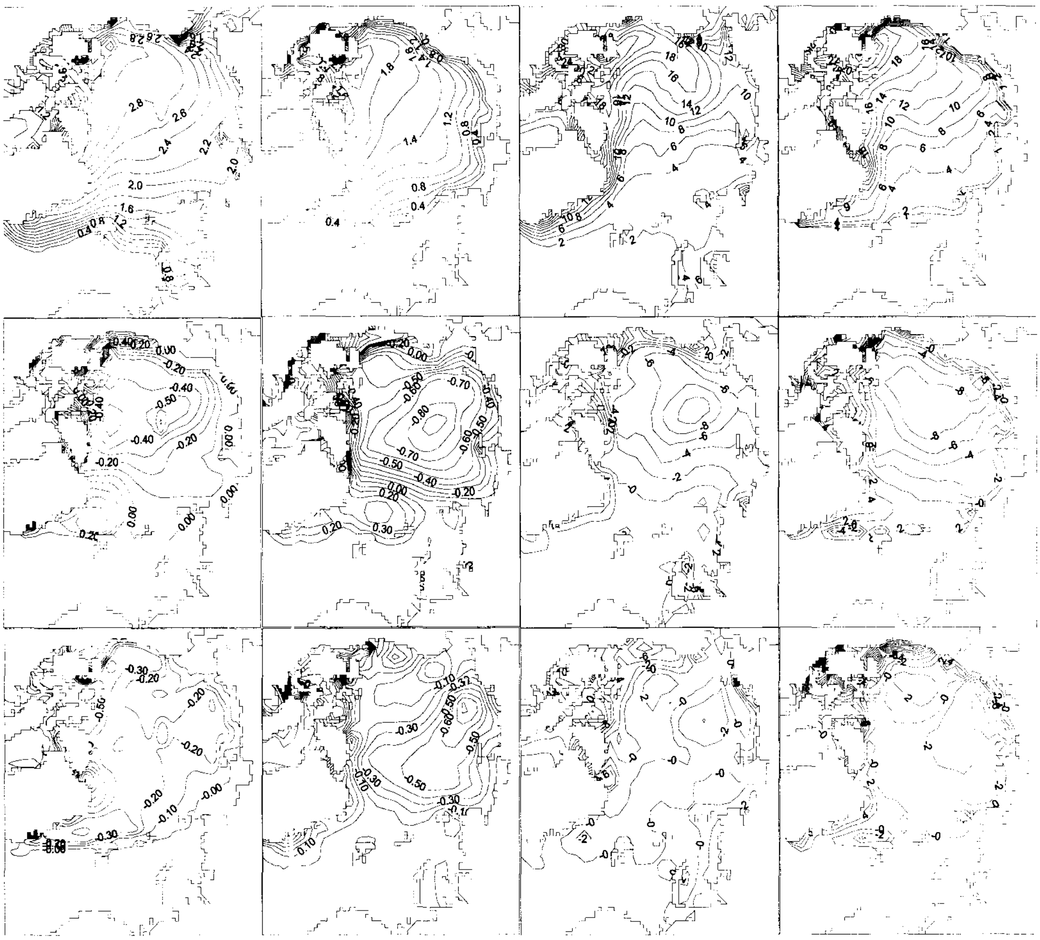

1 2 3 4

Figure 1: Spatial distributions of level sea ice thickness (m) and ridges (number per km^2) in May (1,3) and September (2,4). Upper row represents mean values of parameters averaged for 1984-1988; second row – the differences between values of corresponding parameters averaged for 1989-1993 and 1984-1988; third row – the same but for 1999-2001 and 1984-1988.

4 Application of the model results to navigation in the Arctic

It is well known that the main obstacle for navigation in the Arctic Ocean, the best trade way from Asia to Europe, is the presence of drifting and fast sea ice. Even navigation along the Northern Sea Route, the most investigated and convenient way, is rather complicate and relative unpredictable from point of view duration and cost of voyage. It is despite the existence of powerful nuclear icebreakers and the long period of exploration.

Same time there are many speculations about possibilities to use not only the Northern Sea Route but also the North-West Passage for commercial navigation in nearest future. It bases on some model estimations or extrapolations of described in part 3 the decrease sea ice cover in early 1990th. The results of our model calculations for 1999-2001 (Figure 1, 2) do not confirm such optimistic expectations.

Together with data about level ice thickness and ice concentration the information about ridges, the main obstacles for navigation in ice-covered seas, is very important. Usually it is presented by number of ridges per unit of length or by relative area occupied by ridges from observations (Boradachev et al, 1994). We introduce the new parameter: ridge free navigation index (RFNI). RFNI is a probability of meeting no ridges on the unit of length under conditions of isotropic and chaotic distribution of ridges with fixed length

$$RFNI = (1 - \frac{l}{\pi a})^{2N} \qquad (5)$$

where l is characteristic length of ridge, a is unit of length of the linear displacement, N is ridge concentration.

Formula (5) was obtained as a generalization of classical Buffoon problem. Despite some restrictions, related to peculiarities of ridges space distribution (Dawis and Wadhams, 1995), it could be useful objective index for forecast of navigation conditions with prognostic numerical models, usually producing relative areas of different sea ice characteristics. RFNI allows converting the data about areal distribution to linear, important for planning of navigation.

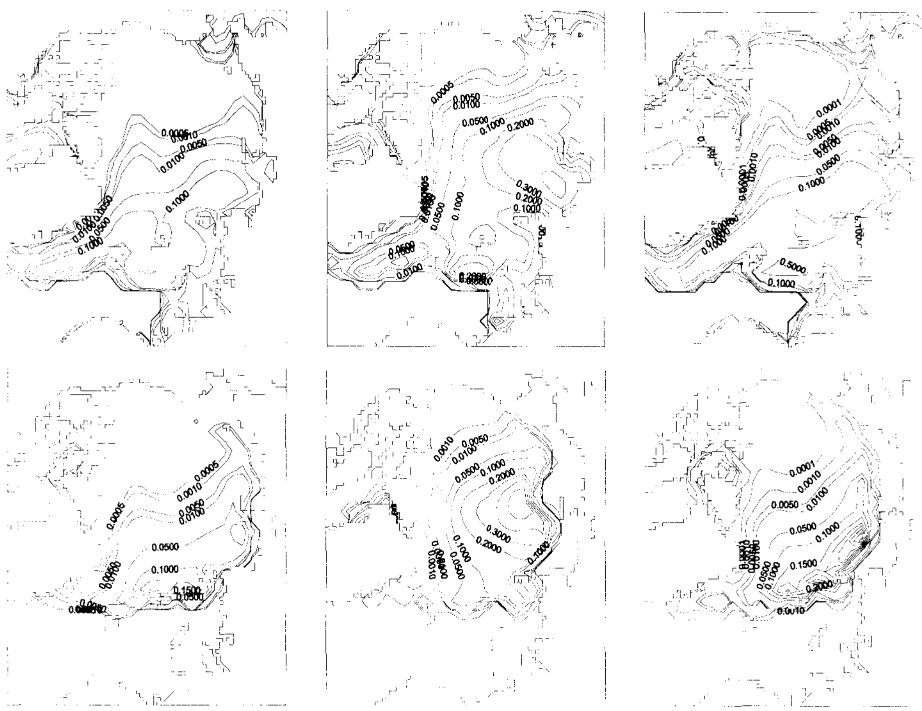

Figure 2: Spatial distributions of RFNI in May (upper panel) and September (low panel) averaged for 1984-1988 (first column), 1989-1993 (second column), and 1999-2001 (third column).

Figure 2 demonstrates the spatial distribution of RFNI during three investigated periods. The most favorable ice conditions for navigation during 1989-1993 years are evident. That period RFNI exceeded value 0.1 on the half of the Arctic Ocean. But it time RFNI remained very low in the Canadian Arctic, supported suggestion about problematic to use the North-West Passage in future, especially taken into account the worsening, follow our model results, of ice conditions in the region in the begin of recent century.
To investigate the long-term variability of sea ice conditions along the Northern Sea Route in May, the most difficult month for navigation, we choose 4 points in the central parts of the Kara, Laptev, East-Siberian, and Chukchi Seas (Figure 3). For these points from model results were extracted values characterized the state of sea ice during all investigated period. Figures 3b-3e present 5 years moving average data about level sea ice thickness (b), total ice (c) and ridge (d) concentration, and RFNI (e).

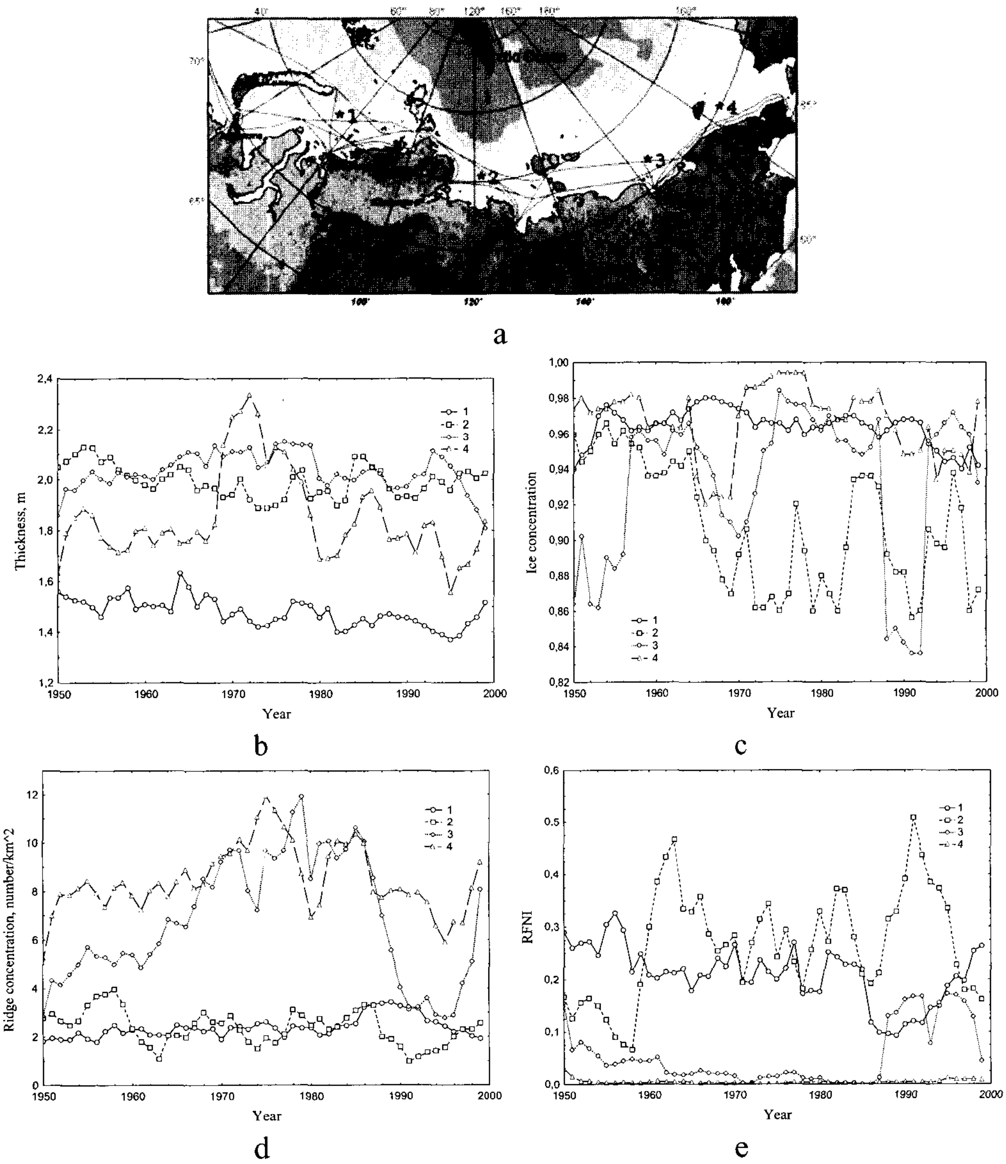

Figure 3: Ice conditions on the Northern Sea Route

As it is possible to see from Figure 3 the modeled characteristics of sea ice cover do not demonstrated any significant trends during 1950 – 2000 years. It times there is the strong interannual variability, especially of ridge concentration and RFNI, in the Laptev, East-Siberian and Chukchi Seas. The open northern boundaries of these seas situate on the south periphery of the Beaufort Gyre and undergo the strong influence of the ice drift in the Canadian region of the Arctic Basin. In turn ice drift in this region, depends on peculiarities of atmospheric circulation (cyclonic or anticyclonic). As a result we have the dominant increase of ridge concentration and decrease of RFNI from 1950^{th} to 1980^{th}, strong decrease of first and increase of second parameters in early 1990^{th}, and return to previous values during late 1990^{th}. In the Kara Sea the modest negative trends of level sea thickness and ice concentration could be noticed, as well increase of RFNI in 1990^{th}. The weak negative correlation between characteristics of sea ice cover in this sea with the same in others, known as "ice opposition" could be marked.

5 Conclusions

An original dynamic–thermodynamic sea ice model satisfactorily reproduces the main characteristics of sea ice cover and sea ice extent in the Arctic Basin and its decrease in early 1990th. At times model allows to suppose the partial recovery of sea ice cover in the Canadian region of the Arctic Ocean in the end of twenty century. The employment of explicit form for description of ridging gave opportunity to assume that the observed ice thinning is the result of reduction the intensity of ridging processes. Introduced Ridge Free Navigation Index (RFNI), allowing to transform information about spatial distribution of ridges from model to linear characteristic, important for planning of ship route, gives possibility to estimate long-term variability of probability the ridge free navigation in the different parts of the Arctic Ocean including the Northern Sea Route area.

Acknowledgements

We are grateful to the International Arctic Research Center, University of Alaska Fairbanks (USA), Hokkaido University, Sapporo, (Japan), Arctic and Antarctic Research Institute (St.-Petersburg, Russia) and Seoul National University (Korea) for the support in preparation this paper. Frontier Research System for Global Change and NTP of the Russian Ministry of Industry and Science funded this research.

References

Belotserkovskii, O.M. 1984. Numerical Modeling in Mechanics of Continuous Medium (in Russian), Nauka, Moscow 519.

Boradachev, V.E., V.P. Gavrilo and M.M. Kazansky. 1994. Dictionary of Sea Ice Terminology (in Russian)., Gidrometeoizdat, SPb, 125.

Burden R.P., G.W. Timco. 1995. Catalogue of sea ice ridges. –Technical report, Canada, 69.

Davis N.R., P. Wadhams. 1995. A statistical analysis of Arctic pressure ridge morphology, J. Geophys. Res., **100**, **6**, 10915-10925.

Doronin, Yu.P. 1969. Heat Interaction of Atmosphere and Hydrosphere in the Arctic (in Russian), Gidrometeoizdat, Leningrad 299.

Ebert, E.E. and J.A. Curry. 1993. An intermediate one-dimensional thermodynamic sea ice model for investigating ice-atmosphere interaction, J. Geophys. Res. **98**, 10085–10109.

Flato, G.M. and W.D. Hibler III. 1992. Modeling pack ice as a cavitating fluid, J. Phys. Oceanogr. **22**, 626–651.

Hibler, W.D. and S. Ackley. 1973, A sea ice terrain model and its application to surface vehicle trafficability. U.S. CRREL Research Report RR 314: 20.

Hilmer, M. and P. Lemke. 2000. On the decrease of Arctic sea ice volume, Geophys. Res. Lett. **27**, 3751–3754.

Ikeda, M., J. Wang and A. Makshtas. 2003. Importance of clouds to the decaying trend in the Arctic ice cover. J. Meteorol. Soc. Japan, 179-189.

Jordan, R.E., E.L. Andreas and A.P. Makshtas. 1999. Heat budget of snow-covered sea ice at North Pole 4, J. Geophys. Res. **104**, 7785–7806.

Kalnay, E. and 21 coauthors 1996 The NCEP/NCAR 40-years reanalysis project, Bull. Amer. Meteorol. Soc. 77, 437–471.

Kwok, R. and D.A. Rothrock. 1999. Variability of fram strait ice flux and north atlantic oscillation, J. Geophys. Res., **104**, 5177-5189.

Makshtas A., S. Shoutilin and E. Andreas. 2003. Possible dynamic and thermal causes for the recent decrease in sea ice in the Arctic. J. Ceophys. Res., **108**, 25-1 - 25-13.

Makshtas A., S. Shoutilin and V. Romanov. 2002. Sensitivity of modeled sea ice to external forcing and parameterizations of heat exchange processes. Ice in the Environment, Proc. of the 16th IAHR International Symposium on Ice Dunedin, New Zealand, **2**, 259 - 267.

Maslanik, J.A., A.H. Lynch, M.C. Serreze and W. Wu. 2000. A case study of regional climate anomalies in the Arctic: Performance requirements for a coupled model, J. Climate **13**, 383–401.

Parkinson, C.L., D.J. Cavalieri, P. Gloersen, H.J. Zwally and J.C. Comiso. 1999. Arctic sea ice extents, areas, and trends, 1978-1996, J. Geophys. Res., **104**, 20837-20856.

Polyakov, I. and M. Johnson. 2000. Decadal and interdecadal arctic ocean variability, Geophys. Res. Lett., **27**, 4097-4100.

Proshutinsky, A.Y., and M.A. Johnson. 1997. Two circulation regimes of the wind-driven Arctic Ocean, J. Geophys. Res., **102**, 12493-12514.

Rothrock, D.A., J. Zhang and Y. Yu. 2003, The arctic ice thickness anomaly of the 1990s: A consistent view from observations and models, J. Geophys. Res., **108**, 28-1 – 28-10.

Rothrock, D.A., Y. Yu and G.A. Maykut. 1999. Thinning of the Arctic sea-ice cover, Geophys. Res. Lett. **26**, 3469–3472.

Semtner, A.J., Jr. 1976. A model for the thermodynamic growth of sea ice in numerical investigations of climate, J. Phys. Oceanogr., **6**, 379–389.

Thorndike, A.S., D.A. Rothrock, G.A. Maykut and R. Colony. 1975. The thickness distribution of sea ice, J. Geophys. Res., **80**, 4501-4513.

Thorndike, A.S. 1992. A toy model linking atmospheric thermal radiation and sea-ice growth, J. Geophys. Res., **97**, 9401-9410.

Tucker W.B., J.W. Weatherly, D.T. Eppler, D. Farmer and D.L. Bentley. 2001. Evidence for the rapid thinning of sea ice in the western Arctic Ocean at the end of the 1980s, Geophys. Res. Lett., **28**, 2851-2854.

Walsh, J.E., W.E. Chapman and T.L. Shy. 1996. Recent decrease of sea level pressure in the central Arctic, J. Climate, **9**, 480-486.

Warren, S.G., I.G. Rigor, N. Untersteiner, V.F. Radionov, N.N. Bryazgin, Y.I. Alexandrov and R. Colony. 1999. Snow depth on Arctic sea ice, J. Climate, **12**, 1814-1829.

Winsor, P. 2001. Arctic sea ice thickness remained constant during the 1990s, Geophys. Res. Lett., **28**, 1039-1041.